https://doi.org/10.5194/acp-2021-230
Preprint. Discussion started: 16 March 2021

Atmospheric Chemistry and Physics Discussions

Gas-particle partitioning of polyol tracers in the western Yangtze River Delta, China: Absorptive or Henry's law partitioning?

Chao Qin[a], Yafeng Gou[b], Yuhang Wang[c], Yuhao Mao[b], Hong Liao[b], Qin'geng Wang[d], Mingjie Xie[b,*]

[a] Colleges of Resources and Environmental Sciences, Nanjing Agricultural University, Nanjing 210095, China

[b] Collaborative Innovation Center of Atmospheric Environment and Equipment Technology, Jiangsu Key Laboratory of Atmospheric Environment Monitoring and Pollution Control, School of Environmental Science and Engineering, Nanjing University of Information Science & Technology, 219 Ningliu Road, Nanjing 210044, China

[c] School of Earth and Atmospheric Sciences, Georgia Institute of Technology, Atlanta, GA 30332

[d] State Key Laboratory of Pollution Control and Resources Reuse, School of the Environment, Nanjing University, Nanjing 210023, China

*Corresponding to:

Mingjie Xie (mingjie.xie@nuist.edu.cn; mingjie.xie@colorado.edu);

Tel: +86-18851903788l; Fax: +86-25-58731051;

Mailing address: 219 Ningliu Road, Nanjing, Jiangsu, 210044, China

https://doi.org/10.5194/acp-2021-230
Preprint. Discussion started: 16 March 2021

Atmospheric Chemistry and Physics Discussions

Abstract

Gas-particle partitioning of water-soluble organic compounds plays a significant role in the formation and source apportionment of organic aerosols, but is poorly characterized. In this work, gas- and particle-phase concentrations of isoprene oxidation products (C5-alkene triols and 2-methylterols), levoglucosan, and sugar polyols were measured simultaneously at a suburban site of the western Yangtze River Delta in east China. All target polyols were primarily distributed into the particle phase (85.9 – 99.8%), and their average particle-phase fractions were not strictly dependent on vapor pressures. Moreover, the measurement-based partitioning coefficients ($K_{p,OM}$) of isoprene oxidation products and levoglucosan were 10^2 to 10^4 times larger than their predicted $K_{p,OM}$ based on the equilibrium absorptive partitioning model. These are likely attributed to the hygroscopic properties of polyol tracers and high aerosol liquid water (ALW) concentrations (~20 µg m^{-3}) of the study location. Due to the large gaps (up to 10^7) between measurement-based effective Henry's law coefficients ($K_{H,e}$) and predicted values in pure water ($K_{H,w}$), the gas-particle partitioning of polyol tracers could not be depicted using Henry's law alone either. The regressions of log ($K_{H,w}/K_{H,e}$) versus molality of major water-soluble components in ALW indicated that sulfate ions ("salting-in effect") and water-soluble organic carbon can promote the partitioning of polyol tracers into the aqueous phase. These results suggest a partitioning mechanism of enhanced aqueous-phase uptake for polyol tracers, which partly reveals the discrepancy between observation and modeling of secondary organic aerosols.

https://doi.org/10.5194/acp-2021-230
Preprint. Discussion started: 16 March 2021

1 Introduction

The water-soluble organic carbon (WSOC) documented for ambient aerosols can account for 20-80% of particulate organic matter based on carbon mass (Saxena and Hildemann, 1996; Kondo et al., 2007). Filed studies on the hygroscopic growth and cloud condensation nucleus (CCN) activity of aerosol extracts indicated that WSOC contributed significantly to aerosol hygroscopicity, and modified the hydration behavior of inorganic species (e.g., sulfate, nitrate, and ammonium; Hallar et al., 2013; Taylor et al., 2017). Thus, WSOC plays an important role in changing radiative and cloud nucleating properties of atmospheric particles. Particulate WSOC is a complex mixture of polar organic compounds containing oxygenated functional groups (e.g., hydroxyl, carboxyl, and carbonyl groups), among which a list of organic compounds with multiple hydroxyl (polyols) groups have been identified using gas chromatography (GC)-mass spectrometry (MS) and linked with specific emission sources. For example, C5-alkene triols and 2-methyltetrols are isoprene oxidation products (Claeys et al., 2004; Wang et al., 2005; Surratt et al., 2006); levoglucosan is a typical pyrolysis product of cellulose (Simoneit et al., 1999); primary saccharides (e.g., fructose and glucose) and saccharide polyols (e.g., arabitol and mannitol) are commonly associated with soil microbiota and fungal spores, respectively (Simoneit et al., 2004; Bauer et al., 2008).

To quantify the sources contributing to WSOC, concentrations of individual organic tracers are often used as inputs for receptor-based modeling (Zhang et al., 2009; Hu et al., 2010). Due to the influences of gas-particle partitioning on source apportionment, Xie et al. (2013, 2014c) suggested the involvement of gas-phase concentrations of organic makers through theoretical prediction or field measurements. The equilibrium absorptive partitioning theory outlined by Pankow (1994a, b) and

https://doi.org/10.5194/acp-2021-230
Preprint. Discussion started: 16 March 2021

laboratory measurements of secondary organic aerosol (SOA) yields (Odum et al., 1996) have been widely applied to predict SOA formation in traditional modeling studies (Heald et al., 2005; Volkamer et al., 2006; Hodzic et al., 2010). The large discrepancy between modeled and observed SOA loadings might be partly explained by the fact that the newly generated SOA did not undergo gas-phase oxidation followed by absorptive partitioning (Jang et al., 2002; Kroll et al., 2005; Perraud et al., 2012). Unlike non-polar species such as *n*-alkanes and polycyclic aromatic hydrocarbons (PAHs) that are well simulated (Simcik et al., 1998; Xie et al., 2014a), the absorptive partitioning model underestimated particle-phase concentrations of carbonyls by several orders of magnitude (Healy et al., 2008; Kampf et al., 2013; Shen et al., 2018;). Zhao et al. (2013) observed a positive dependence of particle-phase pinonaldehyde on relative humidity (RH, %), and inferred that aerosol water favored the formation of pinonaldehyde in the atmosphere. However, every few studies have been performed on the measurement of gaseous polyols (Xie et al., 2014b; Isaacman-VanWertz et al., 2016), and their gas-particle partitioning were poorly understood.

Henry's law can depict the uptake of a compound into a liquid, highly dilute solution in (e.g., cloud droplets) the atmosphere (Ip et al., 2009; Compernolle and Müller, 2014a). Aerosol water is also a major component of atmospheric particles, and accounts for 40% by volume at 50% RH in Europe (Tsyro, 2005). But the bulk aerosol solution is highly concentrated with inorganic ions and WSOC. Both laboratory and field studies observed enhanced effective Henry's law coefficients (K^{e}_{H}, mol m^{-3} atm^{-1}) of carbonyl compounds with inorganic salt concentrations (in mol kg^{-1} aerosol liquid water content, ALWC; Kampf et al., 2013; Waxman et al., 2015; Shen et al., 2018). This termed "salting-in" effect (Setschenow, 1889) is not mechanistically understood,

https://doi.org/10.5194/acp-2021-230
Preprint. Discussion started: 16 March 2021

and might be linked with the hydrophilic interactions (e.g., hydrogen bonding) between polar organic compounds and inorganic ions leading to an increase of entropy or decrease of Gibbs free energy (Almeida et al., 1983; Waxman et al., 2015). Polyol tracers are highly water-soluble and their gas-particle partitioning is very likely driven by the aqueous phase containing substantial ionic species in ambient aerosols. In the Southeastern US, the particle-phase fraction of WSOC is highly dependent on RH and ALWC (Hennigan et al., 2009).

In the present study, polyols related to specific emission sources in gaseous and particle phases were measured concurrently in northern Nanjing, China. The sampling and chemical analysis were performed in a similar manner as Xie et al. (2014b), while an additional step was added prior to GC-MS analysis to clean the extracts of gaseous samples. The absorptive and Henry's law partitioning coefficients of polyol tracers were calculated based on measurements and predicted theoretically for comparison. Finally, the effects of water-soluble inorganic ions and WSOC on the partitioning of atmospheric polyols were evaluated. This work unveils the gas-particle partitioning of polyols at a suburban site in eastern China, where the estimated average mass concentration of aerosol liquid water is close to 20 μg m^{-3} (Yang et al., 2021). The results will benefit future studies on modeling and source apportionment of organic aerosols.

2 Methods

2.1 Field Sampling

Details of the sampling information were provided in Yang et al. (2021). Briefly, ambient air was sampled on the rooftop of a seven-story library building located in Nanjing University of Information Science and Technology (NUIST 32.21 °N, 118.71

https://doi.org/10.5194/acp-2021-230
Preprint. Discussion started: 16 March 2021

^{o}E), a suburban site in the western Yangtze River Delta of east China. A medium volume sampler (PM-PUF-300, Mingye Environmental, Gugangzhou, China) equipped with a 2.5 µm cut impactor was configured to collect particulate matter with aerodynamic diameter less than 2.5 µm ($PM_{2.5}$) and gaseous organic compounds at a flow rate of 300 L min^{-1}. After the impactor, the sampled air flowed through a filter pack containing two stacked pre-baked (550 ^{o}C, 4 h) quartz filters (20.3 cm × 12.6 cm, Munktell Filter AB, Sweden) and a polyurethane foam (PUF, 65 mm diameter × 37.5 mm length) cartridge in series. The top quartz filter (Q_f) in the filter pack was loaded with $PM_{2.5}$; gaseous organic compounds adsorbed on the backup quartz filter (Q_b) was determined to evaluate sampling artifacts ("blow on" and "blow off" effects); and the PUF cartridge was used for the sampling of gaseous polyols. Xie et al. (2014b) demonstrated that using bare PUF material could capture gaseous 2-methytetrols and levoglucosan with no-excessive breakthrough (< 33%). Filter and PUF samples were collected every sixth day during daytime (8:00 AM – 7:00 PM) and night time (7:00 PM – 7:00 AM next day), respectively, from 09/28/2018 to 09/28/2019. Collection efficiency of gaseous polyols were examined by performing breakthrough experiments using two PUF plugs during nine sampling intervals. Prior to sampling, PUF adsorbents were cleaned and dried in the same way as Xie et al. (2014b). Field blank filter and PUF materials were collected every 10th sample for contamination adjustment. Filter and PUF samples were sealed in prebaked aluminum foil and glass jars, respectively, at –20 ^{o}C until analysis.

2.2 Chemical Analysis

Bulk speciation. The accumulated $PM_{2.5}$ mass and bulk components including water soluble ions (NH_4^+, SO_4^{2-}, NO_3^-, Ca^{2+}, Mg^{2+}, and K^+), organic (OC) and elemental carbon (EC), and WSOC were measured for each filter sample. Their final concentrations were determined by subtracting measurement results of Q_b from those of Q_f. Concentrations of aerosol liquid water were predicted by ISORROPIA II model involving ambient temperature, RH, and concentration data of NH_4^+, SO_4^{2-}, and NO_3^- under the metastable state. Table S1 lists averages and ranges of ambient temperature, RH, measured $PM_{2.5}$ components, and predicted aerosol liquid water from Yang et al. (2021)

Polyols analysis. Details of the analysis method for gaseous and particulate polyols were provided in supplementary information (Text S1). Briefly, 1/8 of each filter sample was pre-spiked with deuterated internal standard and extracted ultrasonically twice for 15 min in 10–15 mL of methanol and methylene chloride mixture (1:1, v/v). After filtration, rotary evaporation, N_2 blown down to dryness, and reaction with 50 μL of N, O-bis(trimethylsilyl)trifluoroacetamide (BSTFA) containing 1% trimethylchlorosilane (TMCS) and 10 μL of pyridine, the derivatives of polyols were diluted to 400 μL using pure hexane for GC-MS analysis. Pre-spiked PUF samples were Soxhlet extracted using a mixture of 225 mL of methylene chloride and 25 mL of methanol, followed by the same procedures of filter sample pretreatment. Prior to GC-MS analysis, 50 μL of pure water was added to precipitate PUF impurities from the final extract. As shown in Figure S1e, all PUF residues are kept in aqueous phase at the bottom of the vial, while the derivatives of polyol tracers are supposed to be retained in the top clear hexane solution. An aliquot of 2 μL of the supernatant was injected for GC-MS analysis under splitless mode, and an internal standard method with a six-point calibration curve (0.05–5 ng μL^{-1}) was performed to quantify polyols concentrations. In this work, isoprene SOA products, including three C5-alkene triols (cis-2-methyl-

https://doi.org/10.5194/acp-2021-230
Preprint. Discussion started: 16 March 2021

1,3,4-trihydroxy-1-butene, 3-methyl-2,3,4-trihydroxy-1-butene, and trans-2-methyl-1,3,4-trihydroxy-1-butene; abbreviated as C5-alkene 1, 2, and 3) and two 2-methyltetrols (2-methylthreitol and 2-methylerythritol), were quantified using meso-erythritol; other polyols were determined using authentic standards.

Analytical recoveries of target polyols were obtained by adding known amounts of standards to blank sampling materials (quartz filter and PUF), followed by extraction and instrumental analysis identically as ambient samples. Method detection limits (MDL) of individual species were estimated as three times the standard deviation of their concentrations determined from six injections of the lowest calibration standard. Table S2 lists recovery and MDL values of authentic standard compounds. Concentrations of polyols in field blank samples were measured and subtracted from air samples if necessary. To obtain appropriate gas-particle distribution of polyol tracers, their field-blank corrected concentrations in filter and PUF samples were adjusted by recoveries.

Gas-particle separation and breakthrough calculation. Polyol tracers detected in Q_b samples are contributed by both gaseous adsorption and particle-phase evaporation from Q_f samples, while their relative contributions are unknown. Previous studies rarely considered the sampling artifacts of particulate polyols. Xie et al. (2014b) adjusted particle- and gas-phase concentrations of levoglucosan and 2-methyltetrol based on Q_b measurements in two different ways. One assumed that Q_b values were completely attributed to gaseous adsorption; the other presumed equal contributions from gaseous adsorption and Q_f evaporation. However, negligible difference in gas-particle distribution was observed. Thus particle-phase concentrations of polyols in this study were represented by Q_f values, and the gas phase was calculated as the sum of Q_b and

https://doi.org/10.5194/acp-2021-230
Preprint. Discussion started: 16 March 2021

PUF measurements.

The sampling efficiency of target polyols were evaluated by collecting and analyzing tandemly installed PUF plugs during nine sampling intervals. The breakthrough of each polyol was calculated as

$$B = \frac{[\mathrm{PUF}]_{\mathrm{back}}}{[\mathrm{PUF}]_{\mathrm{front}} + [\mathrm{PUF}]_{\mathrm{backup}}} \times 100\% \quad (1)$$

where B is the breakthrough of gaseous sampling, and [PUF] represents the concentration of specific compound in front or backup PUF sample. A value of 33% was typically used to indicate excessive breakthrough (Peters et al., 2000).

Calculations of partitioning coefficients. Here, the calculations of measurement- and theory-based absorptive partitioning coefficients ($K^{\mathrm{m}}_{\mathrm{p,OM}}$ and $K^{\mathrm{t}}_{\mathrm{p,OM}}$, m^3 ug^{-1}) were conducted identically as those in Xie et al. (2013, 2014a, b). The equations and parameters were detailed in supplementary information (Text S2).

As aerosol liquid water plays a significant role in the gas-particle partitioning of water-soluble organic compounds, we proposed an equilibrium mechanism in Figure S2. First, aerosol liquid water and water insoluble OM (WIOM) exist in two separate phases (liquid-liquid phase separation), and WSOC and inorganic ions are totally dissolved in the aqueous phase. The distribution of polyol tracers between aqueous and WIOM phases is simply depicted by their octanol-water partition coefficients (K_{OW})

$$K_{\mathrm{OW}} = \frac{c_{\mathrm{OM}}}{c_{\mathrm{w}}} \quad (2)$$

where c_{OM} and c_{w} are polyols concentrations (ng m^{-3} in solution) in WIOM and aqueous phases; log K_{OW} values of target polyols were given by the Estimation Programs Interface (EPI) Suite developed by the US Environmental Protection Agency and Syracuse Research Corporation in Table S3 (US EPA, 2012). Due to the high water-solubility of target polyols ($K_{\mathrm{OW}} < 0.15$), more than 95% of their particle-phase

https://doi.org/10.5194/acp-2021-230
Preprint. Discussion started: 16 March 2021

Atmospheric Chemistry and Physics Discussions

concentrations were distributed into the aqueous phase. Second, gas-phase polyol tracers are in equilibrium with hydrophobic OM and the aqueous phase, respectively, following absorptive partitioning theory (eqs 1 and 2 in Text S2) and Henry's law (eq 3)

$$K_{\mathrm{H},e} = \frac{\frac{F}{M_i}}{\frac{A}{M_i} \times R \times T \times \frac{c_{\mathrm{ALW}}}{\rho_{\mathrm{w}}}} = \frac{\rho_{\mathrm{w}} \times F}{A \times R \times T \times c_{\mathrm{ALW}}} \quad (3)$$

where $K_{\mathrm{H,e}}$ (mol m^{-3} atm^{-1}) is the measurement-based effective Henry's law coefficient; F and A (ng m^{-3}) represent particle- and gas-phase concentrations of polyol tracers in ambient air; M_i (g mol^{-1}) is the molecular weight of specific compound; R (m^3 atm K^{-1} mol^{-1}) and T (K) are ideal gas constant and ambient temperature, respectively; c_{ALW} (μg m^{-3}) is the mass concentration of aerosol liquid water predicted using ISORROPIA II model; ρ_{w} (1 g cm^{-3}) is water density. For comparison purposes, the Henry's law coefficient in pure water at 25 °C ($K^*_{\mathrm{H,w}}$) was predicted from EPI suite (Table S3), and was adjusted for each sampling interval due to the changes in ambient temperature using van 't Hoff equation (Text S3).

3 Results and discussion

3.1 Method evaluation

In our previous study, PUF/XAD-4 resin/PUF and PUF/XAD-7 resin/PUF adsorbent sandwiches were tested for sampling gaseous 2-methyltetrols and levoglucosan (Xie et al., 2014b). The results of breakthrough experiments suggested that both the two sandwiched composites had high sampling efficiency (close to 100%). Moreover, individual parts of the two types of composites (top PUF, middle XAD-4/XAD-7 resin, and backup PUF) were analyzed for 7 samples, and target compounds were only detected in top PUF. Thus, bare PUF material is suitable for sampling gaseous 2-methyltetrols and levoglucosan.

Although PUF materials were pre-cleaned prior to sampling, a few short-chain polyurethanes or impurities could be dissolved during Soxhlet extraction of target compounds using the mixture of methanol and methylene chloride. These substances precipitated when sample extracts were concentrated (Figure S1a, b), and re-dissolved in BSTFA:TMCS/pyridine and hexane after the derivatization step (Figure S1c, d). In Xie et al. (2014b), an aliquot of 2 μL of the sample extract as shown in Figure S1d was injected for GC-MS analysis. Due to the fact that the dissolved PUF materials did not vaporize at ~300 ^{o}C, the GC inlet liner had to be changed for cleaning every few samples. In this work, 50 μL of pure water was added to separate PUF materials from polyol derivatives in hexane solution. As shown in Figure S1e, all PUF residues were retained in the aqueous solution after liquid-liquid phase separation. This pretreatment step was added for the analysis of gaseous samples to save time for changing and cleaning GC inlet liners. However, the revised method did not improve the recoveries of meso-erythritol and levoglucosan in PUF samples (Table S2) compared to those in Xie et al. (2014b). This is because the dissolved PUF materials should have an impact on the derivatization efficiency of polyol species, and future work is warranted to remove dissolved PUF materials in sample extracts before the derivatization step.

Measurement results of breakthrough samples and the resulting *B* values were shown in Figure S3. C5-alkene triols and 2-methyltetrols were mainly observed in summertime, and levoglucosan was only detected in three pairs of breakthrough samples. Their average *B* values (< 33%) indicated no excessive breakthrough (Figure S3a-c), but were higher than those reported by Xie et al. (2014b). This might be ascribed to the greater face velocity (1.5 cm s^{-1}) for sampling gaseous polyols than that (0.61 cm

https://doi.org/10.5194/acp-2021-230
Preprint. Discussion started: 16 March 2021

s^{-1}) in our previous study. Unlike fructose which had low breakthrough (Figure S3d), glucose and mannitol had comparable concentrations between front and backup PUF samples for several breakthrough experiments (Figure S3e, f), indicating that PUF materials are not suitable for sampling gaseous glucose and mannitol. Mannose and arabitol were not detected or had BDL values for breakthrough samples, and their breakthrough was not provided. In the current work, concentrations of polyol tracers in filter and PUF samples were all reported, but the data of mannose, glucose, arabitol, and mannitol in PUF samples should be treated with caution due to the lack of valid breakthrough results.

3.2 General description of measurement results

Concentrations of individual polyols in Q_f, Q_b, and PUF samples are summarized in Table S4, and their total ambient concentrations (Q_f + Q_b + PUF) are depicted using boxplots in Figure 1. Figure S4 presents temporal variations of total and Q_f concentrations of individual polyols with daytime and night-time measurements distinguished. In general, polyol tracers were predominantly observed on Q_f with averages 1-3 orders of magnitude higher than those on Q_b and PUF. Levoglucosan had the highest average total concentration (66.1 ± 71.1 ng m^{-3}), followed by fructose (15.0 ± 62.9 ng m^{-3}) and mannose (14.3 ± 31.3 ng m^{-3}). C5-alkene triols and 2-methyltetrols are formed from isoprene epoxydiols (IEPOX) under low NO_X conditions (Surratt et al., 2010). All the five species on Q_b were more frequently detected and had average concentrations 2-20 times higher than those in PUF samples. While in Xie et al. (2014b), the sum of 2-methyltetrols in Q_b and adsorbent samples were up to 2.7 times higher than those on Q_f in summer Denver, so isoprene products are not similarly distributed between gas and aerosol phases across different regions. Moreover, isoprene-derived

https://doi.org/10.5194/acp-2021-230
Preprint. Discussion started: 16 March 2021

polyols exhibited prominent elevations in summer (Figure S4a-e), and their daytime concentrations (2.02 ± 3.73 – 10.5 ± 29.3 ng m^{-3}) were only slightly higher than those during night-time (1.63 ± 4.40 – 9.65 ± 32.7 ng m^{-3}). Fu and Kawamura (2011) investigated diurnal variations of polar organic tracers at a forest site in summer by sampling aerosol particles every 4 h. They found that isoprene-derived SOA tracers maximized from later afternoon to early evening. Although no IEPOX will be generated from the oxidation of isoprene by •OH and HO_2• after sunset, the formations of C5-alkene triols and 2-methyltetrols might continue until pre-existing IEPOX is exhausted. This explains the insignificant ($p > 0.05$) day-night differences of C5-alkene triols and 2-methyltetrols in this work.

Levoglucosan was more frequently detected but far less concentrated in PUF than in Q_b samples. Its total concentrations were comparable to those in urban Denver (average 65.3 ± 96.8 ng m^{-3}, range 2.48 – 478 ng m^{-3}), where an average of ~20% partitioned into the gas phase (Xie et al., 2014b). Due to the enhanced biomass burning activities in cold periods for domestic heating at night, levoglucosan showed a clear seasonal pattern (winter maxima and summer minima) and significant ($p = 0.03$) higher concentrations during night-time (Figure S4f). Sugars and sugar alcohols are commonly linked with soil/dust resuspension and associated microbial activities (Simoneit et al., 2004). They were frequently detected in Q_b samples with comparable averages and ranges as those in PUF samples (Table S4). Total concentrations of fructose and glucose were strongly ($r = 0.98$) correlated peaking in middle spring (April 2019, Figure S4h, j), when Ca^{2+} on Q_f also reached its maxima of the year (Yang et al., 2021), indicating an influence from soil/dust resuspension. Arabitol and mannitol had identical seasonal pattern ($r = 0.89$) with elevated total concentrations from May to October (Figure S4i, m), which might be attributed to the high levels of vegetation and autumn decomposing (Burshtein et al., 2011). Multiple peaks of mannose concentrations were observed from spring to autumn, suggesting a variety of contributing sources (e.g., microbial activity, vegetation). Xylitol is likely derived from biomass burning in northern Nanjing due to its strong correlation (r = 0.89) with levoglucosan.

3.3 Gas-particle distribution and absorptive partitioning coefficient

Q_b measurements were often used to assess positive sampling artifacts of particulate OC (Chow et al., 2010; Subramanian et al., 2004), but rarely for particle-phase organic markers. In this study, concentrations of particulate polyols were obtained directly from Q_f measurements, and the gas phase was calculated as the sum of Q_b and PUF values. Figure S5 shows the time series of gas-phase concentrations and particle-phase fractions (F%) of individual polyol tracers. The average F% values of measured species are linearly regressed against the logarithms of their subcooled liquid vapor pressures at 25 °C ($p^{o,*}_L$) in Figure 2. Unlike non-polar organic tracers (e.g., *n*-alkanes and PAHs), some polyols (e.g., 2-methyltetrols and levoglucosan) data did not follow the linear regression line of F% versus log $p^{o,*}_L$. Although gas-phase C5-alkene triols and 2-methyltetrols were majorly observed in summer with significant ($p < 0.05$) day-night variations, their F% values did not show seasonality or day-night difference (p = 0.18-0.73). Other polyols had extremely low concentrations in the gas phase with average F% ranging from 94.2 ± 8.02 – 99.8 ± 1.21%. The average F% values of 2-methyltetrols (87.5 ± 10.6%) and levoglucosan (99.8 ± 1.21%) were greater than those in urban Denver (50–80%; Xie et al., 2014b), where the average sampling temperature (12.5 ± 10.1 °C) was much lower. Thus, the changes in vapor pressures with the ambient temperature might not be the main factor driving gas-particle partitioning of polyol

https://doi.org/10.5194/acp-2021-230
Preprint. Discussion started: 16 March 2021

tracers in northern Nanjing.

To understand if traditional absorptive partitioning theory could be applied to predict the gas-particle partitioning of polyol tracers in northern Nanjing, Table 1 compares log $K^{m}_{p,OM}$ and log $K^{t}_{p,OM}$ of individual compounds. The average $K^{m}_{p,OM}$ values of isoprene SOA tracers, levolgucosan, and meso-erythritol were 10^2 to 10^3 times larger than their corresponding $K^{t}_{p,OM}$. Comparable or even greater (up to 10^5) gap between $K^{m}_{p,OM}$ and $K^{t}_{p,OM}$ has been observed for carbonyls in a number of laboratory and field studies (Healy et al., 2008; Zhao et al., 2013; Shen et al., 2018), which could be ascribed to reactive uptake (e.g., hydration, oligomerization, and esterification) of organic gases onto condensed phase (Galloway et al., 2009). Oligomers, sulfate and nitrate esters of 2-methyltetrols can be formed in the aerosol phase (Surratt et al., 2010), but these products were not expected to dominate particle-phase concentrations of 2-methyltetrols (Lin et al., 2013; Xie et al., 2014b). Although levoglucosan can be readily oxidized by •OH in the aqueous phase of atmospheric particles (Hennigan et al., 2010; Hoffmann et al., 2010), the occurrence of its oligomers, sulfate or nitrate esters was not reported in ambient aerosols. Xie et al. (2014b) found that the gas-particle partitioning of 2-methyltetrols and levoglucosan in urban Denver were highly dependent on the variations in ambient temperature and absorbing organic matter (M_{OM}). While in southeastern US, the particle-phase fractions of isoprene SOA tracers were generally higher than prediction based on absorptive partitioning model (Isaacman-VanWertz et al., 2016). This discrepancy might be related to the spatial heterogeneity of ALWC, which is expected to control the gas-particle partitioning of water-soluble organic matter in the Eastern US (Carlton and Turpin, 2013). In this study, the large difference between $K^{m}_{p,OM}$ and $K^{t}_{p,OM}$ indicated that some mechanisms other than absorptive

https://doi.org/10.5194/acp-2021-230
Preprint. Discussion started: 16 March 2021

partitioning (e.g., Henry's law partitioning) should be involved to predict the gas-particle partitioning of polyol tracers in northern Nanjing, where the ambient particles contained substantial liquid water (21.3 ± 24.2 μg m^{-3}; Table S1).

Unlike isoprene SOA tracers and levoglucosan, the average $K^{t}_{p,OM}$ values of monosaccharides (fructose, mannose, and glucose) and sugar alcohols (xylitol, arabitol, and mannitol) were up to 10^3 times larger than their $K^{m}_{p,OM}$ (Table 1). This is probably caused by the overestimation of gas-phase concentrations of sugar polyols. The organic matter on Q_b is mainly composed of volatile and semi-volatile organic compounds. If the concentrations of organic compounds on Q_b were comparable or higher than those on Q_f, their Q_f values should be dominated by positive artifact. As the vapor pressure decreases, the evaporation loss from Q_f samples becomes non-negligible. Note that the magnitude of negative artifacts is unknown and very difficult to assess, and the vapor pressures of monosaccharides and sugar alcohols are mostly < 10^{-10} atm, their concentrations in Q_b and even PUF samples might contain more contributions from negative artifacts than isoprene SOA tracers and levoglucosan. Considering that low-volatile sugar polyols had less stable recoveries (Table S2) and greater breakthrough (Figure S3e, f), caution is warranted in analyzing their $K^{m}_{p,OM}$ values obtained in this study.

Figure S2 presumes that gas-phase polyols are in equilibrium with WIOM and the aqueous phase, respectively. Then concentrations of WIOM [1.4 × (OC-WSOC)] was used to adjust the calculation of absorptive partitioning coefficients ($K^{m}_{p,WIOM}$) based on eq 1 in supplementary information. In comparison to log $K^{m}_{p,OM}$, the average log $K^{m}_{p,WIOM}$ values of isoprene SOA tracers and levoglucosan were much closer to average log $K^{t}_{p,OM}$ (Tables 1 and S5), supporting that the aerosol liquid water should have

https://doi.org/10.5194/acp-2021-230
Preprint. Discussion started: 16 March 2021

significant impacts on gas-particle partitioning of polyol tracers.

3.4 Effective Henry's law coefficient

Table 2 lists the statistics of measurement-based log $K_{H,e}$ and predicted log $K_{H,w}$. The average $K_{H,w}$ values of isoprene SOA tracers, levoglucosan, and meso-erythritols were 2-6 orders of magnitude lower than their corresponding average $K_{H,e}$, indicating that the ambient atmosphere in northern Nanjing favored the condensation of these polyols. Other polyol compounds exhibited less difference between log $K_{H,e}$ and log $K_{H,w}$, which was very likely caused by the overestimation of their gas-phase concentrations. A number of previous studies observed enhanced $K_{H,e}$ of carbonyls with salt concentrations in aqueous solution (Ip et al., 2009; Kampf et al., 2013; Waxman et al., 2015; Shen et al., 2018), and described this "salting-in" effect using

$$\mathrm{Log}\left(\frac{K_{H,w}}{K_{H,e}}\right) = K_s c_{salt} \qquad (4)$$

where K_s is the salting constant, and c_{salt} is the aqueous-phase concentration of salt in mol kg^{-1} ALWC. This equation is originally defined in Setschenow (1889) by plotting log ($K_{H,w}/K_{H,e}$) versus the total salt concentration (mol L^{-1}).

As sulfate has been identified as the major factor influencing the salting effect of carbonyl species (Kroll et al., 2005; Ip et al., 2009), Figure 3 shows modified Setschenow plots for C5-alkene triols, 2-methyltetrols, and levoglucosan, where log ($K_{H,w}/K_{H,e}$) values were regressed to the molality of sulfate ion in aerosol liquid water ($c_{sulfate}$, mol kg^{-1} ALWC). However, log ($K_{H,w}/K_{H,e}$) data deviated from their expected behavior in the modified Setschenow plot at $c_{sulfate}$ > 12 mol kg^{-1} ALWC, which was also observed for glyoxal (Kampf et al., 2013). This might be because the ambient particles did not undergo liquid-liquid phase separation at $c_{sulfate}$ > 12 mol kg^{-1} ALWC, when the average RH (51.5 ± 15.4%) was lower than the lowest deliquescence RH

https://doi.org/10.5194/acp-2021-230
Preprint. Discussion started: 16 March 2021

(61.8%) of major inorganic salts (e.g., NH_4NO_3, $(NH_4)_2SO_4$) in ambient aerosols (Seinfeld and Pandis, 2016), and the corresponding average concentration of aerosol liquid water was only 5.31 ± 4.05 μg m^{-3}. In Figure 3, negative correlations ($p < 0.01$) are observed at $c_{sulfate}$ < 12 mol kg^{-1} ALWC, and the K_s values range from -0.17 to -0.15 kg mol^{-1}. Figure S6 shows the regressions between log ($K_{H,w}/K_{H,e}$) of individual polyols and $c_{sulfate}$ without considering the deviations at high $c_{sulfate}$, and nearly all species exhibit significant negative correlations ($p < 0.01$). These results indicated the "salting-in" effects for polyol tracers in northern Nanjing, and to our knowledge the present study is the first to calculate their $K_{H,e}$ and K_s. Although several studies have estimated Henry's law constants for a variety of polar organic compounds in pure water (e.g., polyols and polyacids; Compernolle and Müller, 2014a, b), salting effects should be considered in describing their gas-particle partitioning in the ambient atmosphere.

The average $K_{H,e}$ values of polyol tracers (10^{13}–10^{15} mol m^{-3} atm^{-1}) in this study were several orders of magnitude larger than those of carbonyls derived from ambient measurements (10^{10}–10^{12} mol m^{-3} atm^{-1}; Shen et al., 2018) and chamber simulations (~10^{11} mol m^{-3} atm^{-1}; Kroll et al., 2005; Volkamer et al., 2006; Galloway et al., 2009). This is because low molecular weight carbonyls (e.g., glyoxal) are much more volatile ($p^{o,*}_L$ > 10^{-2} atm) than our target polyols (Table S3). According to existing studies, the minimum concentrations of gas-phase glyoxal and methylglyoxal in Chinese cities (~0.1 μg m^{-3}; Liu et al., 2020) are magnitudes higher than the averages of polyol tracers in this work, while their particle-phase concentrations are of the same magnitude. The K_s values of polyol tracers from Figures 3 and S5 (-0.17 – -0.037 kg mol^{-1}) are in a similar range as that of glyoxal (-0.24 – -0.04 kg mol^{-1}; Kampf et al., 2013; Shen et al., 2018; Waxman et al., 2015), indicating that the uptake of different water-soluble

https://doi.org/10.5194/acp-2021-230
Preprint. Discussion started: 16 March 2021

organic compounds might be enhanced by sulfate in a similar manner. However, the mechanisms of "salting-in" effects are not fully understood. Kampf et al. (2013) inferred that the enhanced uptake of glyoxal was accompanied by chemical reactions in the aqueous phase (e.g., hydration and oligomerization), and the interactions between SO_4^{2-} and glyoxal monohydrate had negative Gibbs free energy of water displacement (Waxman et al., 2015). The net "salting-in" effect of 1-nitro-2-naphthol in NaF solution was interpreted by postulating hydrogen bonding (Almeida et al., 1983). A direct binding of cations to ether oxygens was proposed to be responsible for the increased solubility of water-soluble polymers (Sadeghi and Jahani, 2012). Due to the complexity of PM composition, the large gap between $K_{H,e}$ and $K_{H,w}$ cannot be closed by the "salting-in" effect alone, which is supported by the negative intercepts of linear regressions in Figure 3. As shown in Figures S7, log ($K_{H,w}/K_{H,e}$) values of polyol tracers also negatively correlate with the aqueous-phase concentrations of WSOC (c_{WSOC}), given that the plots are more scattered at high c_{WSOC}. This dependence might be partly explained using the "like-dissolves-like" rule, and indicate the importance of heterogeneous chemistry in the particle phase (Hennigan et al., 2009). No significant correlation was observed between log ($K_{H,w}/K_{H,e}$) and NH_4^+ or NO_3^- concentrations. Therefore, the bulk WSOC and sulfate ion should play important roles during the condensation of gas-phase polyols, and further research is warranted to explicitly explain these effects.

4 Conclusions and implications

In this work, concentrations of gas- and particle-phase polyol tracers were measured simultaneously in northern Nanjing. The temporal variations of individual compounds were dominated by their particle-phase concentrations. Because receptor-

https://doi.org/10.5194/acp-2021-230
Preprint. Discussion started: 16 March 2021

based models identify and quantify aerosol sources based on inter-sample variability, gas-particle partitioning of polyol tracers should have little influence on source apportionment barely using particle-phase data in northern Nanjing. When it comes to other places (e.g., western US) where the concentration of aerosol liquid water is extremely low, the influence of gas-particle partitioning will still be a concern.

Similar to southeastern US, the ambient atmosphere in northern Nanjing also favored the condensation of polyol tracers, which was ascribed to the significant ALWC in these locations. The large gaps of measured versus predicted $K_{p,OM}$ and K_H implied that the gas-particle partitioning of polyol tracers could not be depicted using equilibrium absorptive partitioning model or Henry's law alone. In addition to the "salting-in" effect primarily due to the sulfate ions, other aerosol components like bulk WSOC might also be responsible for increasing the partitioning of polyol tracers into the condensed phase. So, the results of this study have important implications on the prediction of gas-particle partitioning of water-soluble organics, and further studies are required to explain their enhanced aqueous-phase uptake mechanistically. Due to the hygroscopic properties of highly oxidized organic aerosols, the proposed scheme for gas-particle partitioning of polyol tracers also partly reveals the discrepancy between modeled and observed SOA in previous studies. However, several pre-assumptions (e.g., liquid-liquid phase separation) were made for the proposed gas-particle partitioning scheme in this work, more research is needed to understand the mixing state of inorganic salts, organic components, and aerosol liquid water in atmospheric particles.

Data availability

https://doi.org/10.5194/acp-2021-230
Preprint. Discussion started: 16 March 2021

Data used in the writing of this paper is available at the Harvard Dataverse (https://doi.org/10.7910/DVN/U3IGQR, Qin et al., 2021)

Author contributions

MX designed the research. CQ and YG performed the sampling and chemical analysis. CQ, YM, and MX analyzed the data. CQ and MX wrote the paper with significant contributions from YW, HL, and QW.

Competing interests

The authors declare that they have no conflict of interest.

Acknowledgements

This research was supported by the National Natural Science Foundation of China (NSFC, 41701551). Y. W. was supported by the National Science Foundation Atmospheric Chemistry Program.

References

Almeida, M. B., Alvarez, A. M., Miguel, E. M. D., and Hoyo, E. S. D.: Setchenow coefficients for naphthols by distribution method, Can. J. Chem., 61, 244-248, 10.1139/v83-043, 1983.

Bauer, H., Claeys, M., Vermeylen, R., Schueller, E., Weinke, G., Berger, A., and Puxbaum, H.: Arabitol and mannitol as tracers for the quantification of airborne fungal spores, Atmos. Environ., 42, 588-593, https://doi.org/10.1016/j.atmosenv.2007.10.013, 2008.

Burshtein, N., Lang-Yona, N., and Rudich, Y.: Ergosterol, arabitol and mannitol as tracers for biogenic aerosols in the eastern Mediterranean, Atmos. Chem. Phys., 11, 829-839, 10.5194/acp-11-829-2011, 2011.

Carlton, A. G., and Turpin, B. J.: Particle partitioning potential of organic compounds is highest in the Eastern US and driven by anthropogenic water, Atmos. Chem. Phys., 13, 10203-10214, 10.5194/acp-13-10203-2013, 2013.

Chow, J. C., Watson, J. G., Chen, L. W. A., Rice, J., and Frank, N. H.: Quantification of PM2.5 organic carbon sampling artifacts in US networks, Atmos. Chem. Phys., 10, 5223-5239, 10.5194/acp-10-5223-2010, 2010.

Claeys, M., Graham, B., Vas, G., Wang, W., Vermeylen, R., Pashynska, V., Cafmeyer, J., Guyon, P., Andreae, M. O., Artaxo, P., and Maenhaut, W.: Formation of secondary organic aerosols through photooxidation of isoprene, Science, 303, 1173-1176, 10.1126/science.1092805, 2004.

Compernolle, S., and Müller, J. F.: Henry's law constants of polyols, Atmos. Chem. Phys., 14, 12815-12837, 10.5194/acp-14-12815-2014, 2014a.
Compernolle, S., and Müller, J. F.: Henry's law constants of diacids and hydroxy polyacids: recommended values, Atmos. Chem. Phys., 14, 2699-2712, 10.5194/acp-14-2699-2014, 2014b.
Fu, P., and Kawamura, K.: Diurnal variations of polar organic tracers in summer forest aerosols: A case study of a Quercus and Picea mixed forest in Hokkaido, Japan, Geochem. J., 45, 297-308, 10.2343/geochemj.1.0123, 2011.
Galloway, M. M., Chhabra, P. S., Chan, A. W. H., Surratt, J. D., Flagan, R. C., Seinfeld, J. H., and Keutsch, F. N.: Glyoxal uptake on ammonium sulphate seed aerosol: reaction products and reversibility of uptake under dark and irradiated conditions, Atmos. Chem. Phys., 9, 3331-3345, 10.5194/acp-9-3331-2009, 2009.
Hallar, A. G., Lowenthal, D. H., Clegg, S. L., Samburova, V., Taylor, N., Mazzoleni, L. R., Zielinska, B. K., Kristensen, T. B., Chirokova, G., McCubbin, I. B., Dodson, C., and Collins, D.: Chemical and hygroscopic properties of aerosol organics at Storm Peak Laboratory, J. Geophys. Res. Atmos., 118, 4767-4779, https://doi.org/10.1002/jgrd.50373, 2013.
Heald, C. L., Jacob, D. J., Park, R. J., Russell, L. M., Huebert, B. J., Seinfeld, J. H., Liao, H., and Weber, R. J.: A large organic aerosol source in the free troposphere missing from current models, Geophys. Res. Lett., 32, L18809, https://doi.org/10.1029/2005GL023831, 2005.
Healy, R. M., Wenger, J. C., Metzger, A., Duplissy, J., Kalberer, M., and Dommen, J.: Gas/particle partitioning of carbonyls in the photooxidation of isoprene and 1,3,5-trimethylbenzene, Atmos. Chem. Phys., 8, 3215-3230, 10.5194/acp-8-3215-2008, 2008.
Hennigan, C. J., Bergin, M. H., Russell, A. G., Nenes, A., and Weber, R. J.: Gas/particle partitioning of water-soluble organic aerosol in Atlanta, Atmos. Chem. Phys., 9, 3613-3628, 10.5194/acp-9-3613-2009, 2009.
Hennigan, C. J., Sullivan, A. P., Collett Jr, J. L., and Robinson, A. L.: Levoglucosan stability in biomass burning particles exposed to hydroxyl radicals, Geophys. Res. Lett., 37, L09806, https://doi.org/10.1029/2010GL043088, 2010.
Hodzic, A., Jimenez, J. L., Madronich, S., Canagaratna, M. R., DeCarlo, P. F., Kleinman, L., and Fast, J.: Modeling organic aerosols in a megacity: potential contribution of semi-volatile and intermediate volatility primary organic compounds to secondary organic aerosol formation, Atmos. Chem. Phys., 10, 5491-5514, 10.5194/acp-10-5491-2010, 2010.
Hoffmann, D., Tilgner, A., Iinuma, Y., and Herrmann, H.: Atmospheric stability of levoglucosan: A detailed laboratory and modeling study, Environ. Sci. Technol., 44, 694-699, 10.1021/es902476f, 2010.
Hu, D., Bian, Q., Lau, A. K. H., and Yu, J. Z.: Source apportioning of primary and secondary organic carbon in summer PM2.5 in Hong Kong using positive matrix factorization of secondary and primary organic tracer data, J. Geophys. Res. Atmos., 115, D16204, https://doi.org/10.1029/2009JD012498, 2010.
Ip, H. S. S., Huang, X. H. H., and Yu, J. Z.: Effective Henry's law constants of glyoxal, glyoxylic acid, and glycolic acid, Geophys. Res. Lett., 36, L01802, https://doi.org/10.1029/2008GL036212, 2009.
Isaacman-VanWertz, G., Yee, L. D., Kreisberg, N. M., Wernis, R., Moss, J. A., Hering, S. V., de Sá, S. S., Martin, S. T., Alexander, M. L., Palm, B. B., Hu, W., Campuzano-Jost, P., Day, D. A., Jimenez, J. L., Riva, M., Surratt, J. D., Viegas, J., Manzi, A., Edgerton, E., Baumann, K., Souza, R., Artaxo, P., and Goldstein, A. H.: Ambient gas-particle partitioning of tracers for biogenic oxidation, Environ. Sci. Technol., 50, 9952-9962, 10.1021/acs.est.6b01674, 2016.
Jang, M., Czoschke, N. M., Lee, S., and Kamens, R. M.: Heterogeneous atmospheric aerosol production by acid-catalyzed particle-phase reactions, Science, 298, 814, 10.1126/science.1075798, 2002.
Kampf, C. J., Waxman, E. M., Slowik, J. G., Dommen, J., Pfaffenberger, L., Praplan, A. P., Prévôt, A. S. H., Baltensperger, U., Hoffmann, T., and Volkamer, R.: Effective Henry's law partitioning and the salting constant of glyoxal in aerosols containing sulfate, Environ. Sci. Technol., 47, 4236-4244, 10.1021/es400083d, 2013.
Kondo, Y., Miyazaki, Y., Takegawa, N., Miyakawa, T., Weber, R. J., Jimenez, J. L., Zhang, Q., and Worsnop, D. R.: Oxygenated and water-soluble organic aerosols in Tokyo, J. Geophys. Res. Atmos., 112, D01203, 10.1029/2006jd007056, 2007.
Kroll, J. H., Ng, N. L., Murphy, S. M., Varutbangkul, V., Flagan, R. C., and Seinfeld, J. H.: Chamber studies of secondary organic aerosol growth by reactive uptake of simple carbonyl compounds, J. Geophys. Res. Atmos., 110, D23207, https://doi.org/10.1029/2005JD006004, 2005.
Lin, Y. H., Knipping, E. M., Edgerton, E. S., Shaw, S. L., and Surratt, J. D.: Investigating the influences

https://doi.org/10.5194/acp-2021-230
Preprint. Discussion started: 16 March 2021

of SO2 and NH3 levels on isoprene-derived secondary organic aerosol formation using conditional sampling approaches, Atmos. Chem. Phys., 13, 8457-8470, 10.5194/acp-13-8457-2013, 2013.

Liu, J., Li, X., Li, D., Xu, R., Gao, Y., Chen, S., Liu, Y., Zhao, G., Wang, H., Wang, H., Lou, S., Chen, M., Hu, J., Lu, K., Wu, Z., Hu, M., Zeng, L., and Zhang, Y.: Observations of glyoxal and methylglyoxal in a suburban area of the Yangtze River Delta, China, Atmos. Environ., 238, 117727, https://doi.org/10.1016/j.atmosenv.2020.117727, 2020.

Odum, J. R., Hoffmann, T., Bowman, F., Collins, D., Flagan, R. C., and Seinfeld, J. H.: Gas/particle partitioning and secondary organic aerosol yields, Environ. Sci. Technol., 30, 2580-2585, 10.1021/es950943+, 1996.

Pankow, J. F.: An absorption model of the gas/aerosol partitioning involved in the formation of secondary organic aerosol, Atmos. Environ., 28, 189-193, 10.1016/1352-2310(94)90094-9, 1994a.

Pankow, J. F.: An absorption model of gas/particle partitioning of organic compounds in the atmosphere, Atmos. Environ., 28, 185-188, 10.1016/1352-2310(94)90093-0, 1994b.

Perraud, V., Bruns, E. A., Ezell, M. J., Johnson, S. N., Yu, Y., Alexander, M. L., Zelenyuk, A., Imre, D., Chang, W. L., Dabdub, D., Pankow, J. F., and Finlayson-Pitts, B. J.: Nonequilibrium atmospheric secondary organic aerosol formation and growth, Proc. Natl. Acad. Sci. U.S.A., 109, 2836-2841, 10.1073/pnas.1119909109, 2012.

Peters, A. J., Lane, D. A., Gundel, L. A., Northcott, G. L., and Jones, K. C.: A comparison of high volume and diffusion denuder samplers for measuring semivolatile organic compounds in the atmosphere, Environ. Sci. Technol., 34, 5001-5006, 10.1021/es000056t, 2000.

Qin, C., Gou, Y., Wang, Y., Mao, Y., Liao, H., Wang, Q. g., and Xie, M.: Replication Data for: Gas-particle partitioning of polyol tracers in the western Yangtze River Delta, China, in, V1 ed., Harvard Dataverse, https://doi.org/10.7910/DVN/U3IGQR, 2021.

Sadeghi, R., and Jahani, F.: Salting-in and salting-out of water-soluble polymers in aqueous salt solutions, J. Phys. Chem. B, 116, 5234-5241, 10.1021/jp300665b, 2012.

Saxena, P., and Hildemann, L.: Water-soluble organics in atmospheric particles: A critical review of the literature and application of thermodynamics to identify candidate compounds, J. Atmos. Chem., 24, 57-109, 10.1007/bf00053823, 1996.

Seinfeld, J. H., and Pandis, S. N.: Atmospheric chemistry and physics: from air pollution to climate change, John Wiley & Sons, 2016.

Setschenow, J.: Über die Konstitution der Salzlösungen auf Grund ihres Verhaltens zu Kohlensäure, Z. Phys. Chem., 4U, 117-125, https://doi.org/10.1515/zpch-1889-0409, 1889.

Shen, H., Chen, Z., Li, H., Qian, X., Qin, X., and Shi, W.: Gas-particle partitioning of carbonyl compounds in the ambient atmosphere, Environ. Sci. Technol., 52, 10997-11006, 10.1021/acs.est.8b01882, 2018.

Simcik, M. F., Franz, T. P., Zhang, H., and Eisenreich, S. J.: Gas-particle partitioning of PCBs and PAHs in the Chicago urban and adjacent coastal atmosphere: States of equilibrium, Environ. Sci. Technol., 32, 251-257, 10.1021/es970557n, 1998.

Simoneit, B. R. T., Schauer, J. J., Nolte, C. G., Oros, D. R., Elias, V. O., Fraser, M. P., Rogge, W. F., and Cass, G. R.: Levoglucosan, a tracer for cellulose in biomass burning and atmospheric particles, Atmos. Environ., 33, 173-182, http://dx.doi.org/10.1016/S1352-2310(98)00145-9, 1999.

Simoneit, B. R. T., Elias, V. O., Kobayashi, M., Kawamura, K., Rushdi, A. I., Medeiros, P. M., Rogge, W. F., and Didyk, B. M.: Sugars dominant water-soluble organic compounds in soils and characterization as tracers in atmospheric particulate matter, Environ. Sci. Technol., 38, 5939-5949, 10.1021/es0403099, 2004.

Subramanian, R., Khlystov, A. Y., Cabada, J. C., and Robinson, A. L.: Positive and negative artifacts in particulate organic carbon measurements with denuded and undenuded sampler configurations special issue of aerosol science and technology on findings from the fine particulate matter supersites program, Aerosol Sci. Tech., 38, 27-48, 10.1080/02786820390229354, 2004.

Surratt, J. D., Murphy, S. M., Kroll, J. H., Ng, N. L., Hildebrandt, L., Sorooshian, A., Szmigielski, R., Vermeylen, R., Maenhaut, W., Claeys, M., Flagan, R. C., and Seinfeld, J. H.: Chemical composition of secondary organic aerosol formed from the photooxidation of isoprene, J. Phys. Chem. A, 110, 9665-9690, 10.1021/jp061734m, 2006.

Surratt, J. D., Chan, A. W. H., Eddingsaas, N. C., Chan, M., Loza, C. L., Kwan, A. J., Hersey, S. P., Flagan, R. C., Wennberg, P. O., and Seinfeld, J. H.: Reactive intermediates revealed in secondary organic aerosol formation from isoprene, Proc. Natl. Acad. Sci. U.S.A., 107, 6640-6645, 10.1073/pnas.0911114107, 2010.

Taylor, N. F., Collins, D. R., Lowenthal, D. H., McCubbin, I. B., Hallar, A. G., Samburova, V., Zielinska, B., Kumar, N., and Mazzoleni, L. R.: Hygroscopic growth of water soluble organic carbon isolated from atmospheric aerosol collected at US national parks and Storm Peak Laboratory, Atmos. Chem. Phys., 17, 2555-2571, 10.5194/acp-17-2555-2017, 2017.

Tsyro, S. G.: To what extent can aerosol water explain the discrepancy between model calculated and gravimetric PM10 and PM2.5?, Atmos. Chem. Phys., 5, 515-532, 10.5194/acp-5-515-2005, 2005.

US EPA: Estimation Program Interface (EPI) Suite. Version v4.11, 2012. United States Environmental Protection Agency, Washington, DC, USA. https://www.epa.gov/tsca-screening-tools/download-epi-suitetm-estimation-program-interface-v411

Volkamer, R., Jimenez, J. L., San Martini, F., Dzepina, K., Zhang, Q., Salcedo, D., Molina, L. T., Worsnop, D. R., and Molina, M. J.: Secondary organic aerosol formation from anthropogenic air pollution: Rapid and higher than expected, Geophys. Res. Lett., 33, L17811, https://doi.org/10.1029/2006GL026899, 2006.

Wang, W., Kourtchev, I., Graham, B., Cafmeyer, J., Maenhaut, W., and Claeys, M.: Characterization of oxygenated derivatives of isoprene related to 2-methyltetrols in Amazonian aerosols using trimethylsilylation and gas chromatography/ion trap mass spectrometry, Rapid Commun. Mass Spectrom., 19, 1343-1351, https://doi.org/10.1002/rcm.1940, 2005.

Waxman, E. M., Elm, J., Kurtén, T., Mikkelsen, K. V., Ziemann, P. J., and Volkamer, R.: Glyoxal and methylglyoxal Setschenow salting constants in sulfate, nitrate, and chloride solutions: Measurements and Gibbs energies, Environ. Sci. Technol., 49, 11500-11508, 10.1021/acs.est.5b02782, 2015.

Xie, M., Barsanti, K. C., Hannigan, M. P., Dutton, S. J., and Vedal, S.: Positive matrix factorization of PM2.5 - eliminating the effects of gas/particle partitioning of semivolatile organic compounds, Atmos. Chem. Phys., 13, 7381-7393, 10.5194/acp-13-7381-2013, 2013.

Xie, M., Hannigan, M. P., and Barsanti, K. C.: Gas/particle partitioning of n-alkanes, PAHs and oxygenated PAHs in urban Denver, Atmos. Environ., 95, 355-362, http://dx.doi.org/10.1016/j.atmosenv.2014.06.056, 2014a.

Xie, M., Hannigan, M. P., and Barsanti, K. C.: Gas/particle partitioning of 2-methyltetrols and levoglucosan at an urban site in Denver, Environ. Sci. Technol., 48, 2835-2842, 10.1021/es405356n, 2014b.

Xie, M., Hannigan, M. P., and Barsanti, K. C.: Impact of gas/particle partitioning of semivolatile organic compounds on source apportionment with positive matrix factorization, Environ. Sci. Technol., 48, 9053-9060, 10.1021/es5022262, 2014c.

Yang, L., Shang, Y., Hannigan, M. P., Zhu, R., Wang, Q. g., Qin, C., and Xie, M.: Collocated speciation of PM2.5 using tandem quartz filters in northern nanjing, China: Sampling artifacts and measurement uncertainty, Atmos. Environ., 246, 118066, https://doi.org/10.1016/j.atmosenv.2020.118066, 2021.

Zhang, Y., Sheesley, R. J., Schauer, J. J., Lewandowski, M., Jaoui, M., Offenberg, J. H., Kleindienst, T. E., and Edney, E. O.: Source apportionment of primary and secondary organic aerosols using positive matrix factorization (PMF) of molecular markers, Atmos. Environ., 43, 5567-5574, https://doi.org/10.1016/j.atmosenv.2009.02.047, 2009.

Zhao, Y., Kreisberg, N. M., Worton, D. R., Isaacman, G., Weber, R. J., Liu, S., Day, D. A., Russell, L. M., Markovic, M. Z., VandenBoer, T. C., Murphy, J. G., Hering, S. V., and Goldstein, A. H.: Insights into secondary organic aerosol formation mechanisms from measured gas/particle partitioning of specific organic tracer compounds, Environ. Sci. Technol., 47, 3781-3787, 10.1021/es304587x, 2013.

https://doi.org/10.5194/acp-2021-230
Preprint. Discussion started: 16 March 2021

Table 1. Statistics for measured and predicted log $K_{p,OM}$ of individual polyol tracers.

Species	No. of obs.	Log $K^{m}_{p,OM}$			Log $K^{t}_{p,OM}$		
		Median	Average	Range	Median	Average	Range
Isoprene SOA tracers							
C5-alkene triol 1	53	0.47	0.33 ± 0.71	-1.30 – 2.61	-3.23	-3.09 ± 0.44	-3.70 – -1.63
C5-alkene triol 2	63	0.19	0.15 ± 0.55	-1.02 – 2.26	-3.70	-3.62 ± 0.37	-4.24 – -2.67
C5-alkene triol 3	83	0.38	0.35 ± 0.68	-1.86 – 2.25	-3.01	-2.90 ± 0.48	-3.70 – -1.63
2-Methylthreitol	101	-0.13	-0.12 ± 0.48	-1.15 – 0.92	-1.90	-1.87 ± 0.52	-2.81 – -0.62
2-Methylerythritol	95	-0.089	-0.011 ± 0.58	-1.09 – 2.06	-1.91	-1.90 ± 0.51	-2.81 – -0.62
Biomass burning tracer							
Levoglucosan	65	2.34	2.23 ± 0.72	-0.11 – 3.36	-0.12	-0.038 ± 0.59	-1.00 – 1.29
Sugars ang sugar alcohols							
Meso-erythritol	31	0.84	0.87 ± 0.53	-0.47 – 1.81	-0.80	-0.65 ± 0.48	-1.35 – 0.69
Fructose	85	0.55	0.65 ± 0.73	-0.96 – 3.01	1.14	1.17 ± 0.62	0.015 – 2.72
Mannose	74	0.57	0.62 ± 0.71	-0.94 – 2.81	1.23	1.28 ± 0.66	0.18 – 2.81
Glucose	88	0.41	0.42 ± 0.67	-1.08 – 1.92	0.31	0.34 ± 0.65	-0.75 – 1.92
Xylitol	22	0.35	0.24 ± 0.54	-1.23 – 0.97	3.43	3.37 ± 0.57	2.11 – 4.39
Arabitol	30	1.40	1.46 ± 0.89	-0.19 – 4.20	3.15	3.25 ± 0.77	2.05 – 4.81
Manitol	65	1.06	1.08 ± 0.63	-0.35 – 2.53	2.31	2.33 ± 0.70	1.15 – 3.98

https://doi.org/10.5194/acp-2021-230
Preprint. Discussion started: 16 March 2021

Atmospheric Chemistry and Physics
Discussions

Table 2. Statistics for log $K_{H,e}$ and log $K_{H,w}$ of individual polyol tracers.

species	No. of obs.	Log $K_{H,e}$			Log $K_{H,w}$		
		Median	Average	Range	Median	Average	Range
Isoprene SOA tracers							
C5-alkene triol 1	53	14.0	13.9 ± 0.86	11.5 – 16.4	7.06	7.22 ± 0.50	6.53 – 8.87
C5-alkene triol 2	63	13.7	13.6 ± 0.73	11.2 – 16.1	7.24	7.34 ± 0.45	6.60 – 8.49
C5-alkene triol 3	83	13.9	13.8 ± 0.85	10.6 – 16.1	7.31	7.43 ± 0.55	6.53 – 8.87
2-Methylthreitol	101	13.4	13.3 ± 0.70	10.9 – 14.8	9.96	10.0 ± 0.80	8.55 – 11.9
2-Methylerythritol	95	13.5	13.5 ± 0.71	11.6 – 15.6	9.93	9.95 ± 0.79	8.55 – 11.9
Biomass burning tracer							
Levoglucosan	65	15.7	15.7 ± 0.90	13.2 – 17.3	13.3	13.4 ± 0.56	12.4 – 14.6
Sugars ang sugar alcohols							
Meso-erythritol	31	14.5	14.4 ± 0.60	12.8 – 15.6	9.44	9.65 ± 0.66	8.68 – 11.5
Fructose	85	14.2	14.1 ± 0.89	11.9 – 16.5	14.6	14.7 ± 0.84	13.1 – 16.8
Mannose	74	14.0	14.1 ± 0.94	12.1 – 16.8	10.9	10.9 ± 0.88	9.46 – 13.0
Glucose	88	13.9	13.9 ± 0.93	11.3 – 16.3	14.6	14.7 ± 0.85	13.2 – 16.8
Xylitol	22	13.8	13.7 ± 0.72	12.6 – 15.0	12.1	12.1 ± 0.62	10.7 – 13.2
Arabitol	30	15.1	15.0 ± 1.23	13.0 – 18.2	11.2	11.4 ± 0.83	10.0 – 13.0
Mannitol	65	14.6	14.5 ± 0.94	12.1 – 16.4	12.9	12.9 ± 1.15	11.0 – 15.6

https://doi.org/10.5194/acp-2021-230
Preprint. Discussion started: 16 March 2021

Atmospheric Chemistry and Physics
Discussions

Figure 1

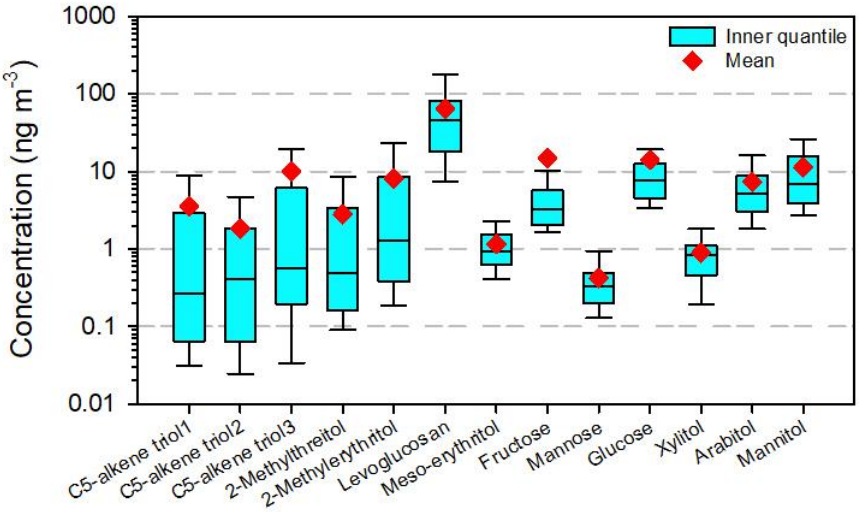

Figure 1. Total concentrations of individual polyols (Q_f + Q_b + PUF) in the ambient atmosphere of northern Nanjing. The boxes depict the median (dark line), inner quantile range (box), 10th and 90th percentiles (whiskers), and the mean (red diamond).

https://doi.org/10.5194/acp-2021-230
Preprint. Discussion started: 16 March 2021

Atmospheric Chemistry and Physics Discussions

Figure 2

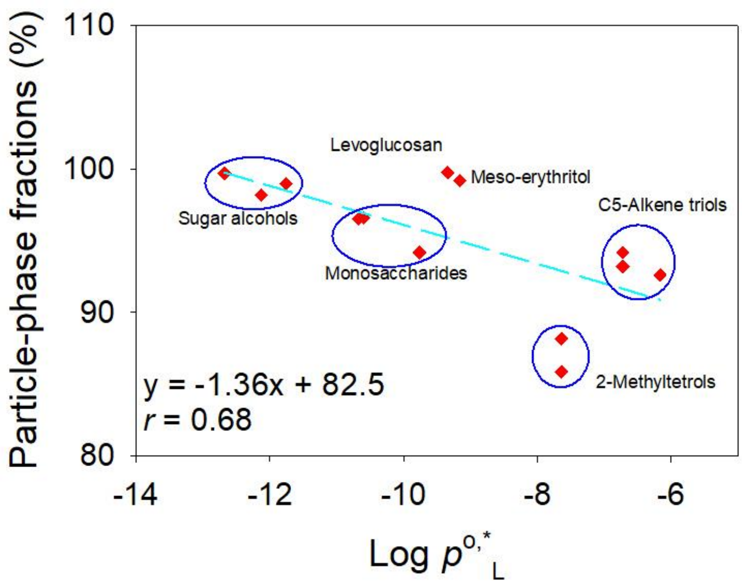

Figure 2. Linear relationship between average aerosol-phase fractions and log $p^{o,*}_L$ of polyol tracers.

https://doi.org/10.5194/acp-2021-230
Preprint. Discussion started: 16 March 2021

Atmospheric Chemistry and Physics
Discussions

Figure 3

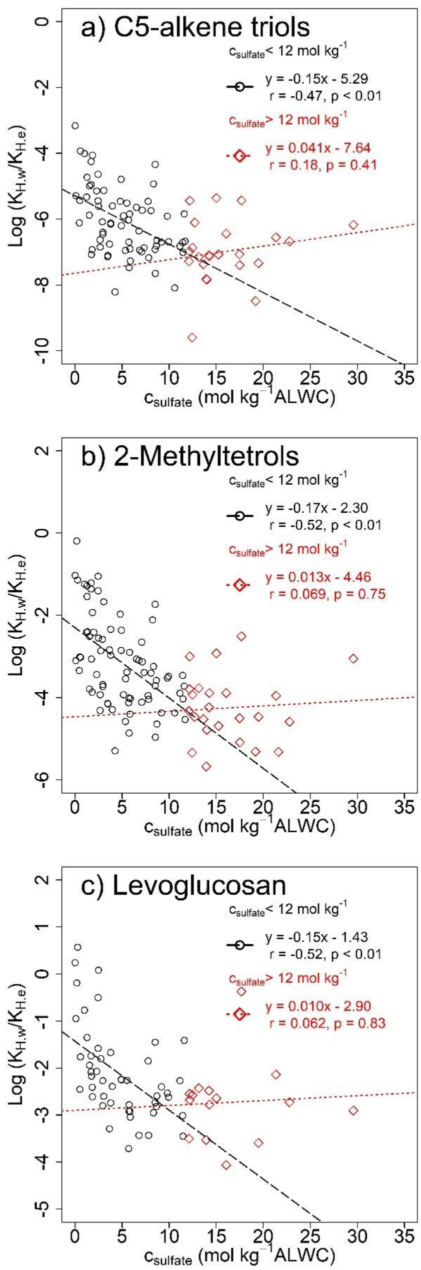

Figure 3. Modified Setschenow plots of log ($K_{H,w}/K_{H,e}$) vs. $c_{sulfate}$ for (a) C5-alkene triols, (b) 2-methyltetrols, and (c) levoglucosan.